Smoothing Low SNR Molecular Images Via Anisotropic Median-Diffusion

Jian Ling[1], *Member, IEEE,* and Alan C. Bovik[2], *Fellow, IEEE*

[1]Southwest Research Institute
Bioengineering Department
6220 Culebra Road
San Antonio, TX 78238-5166, USA
E-mail: jling@swri.edu

[2]Laboratory for Image and Video Engineering (LIVE)
Department of Electrical and Computer Engineering
The University of Texas at Austin, Austin, TX 78712-1084, USA
Email: bovik@ece.utexas.edu

Abstract

We propose a new anisotropic diffusion filter for denoising low signal-to-noise (SNR) molecular images. This filter, which incorporates a median filter into the diffusion steps, is called an anisotropic median-diffusion filter. This hybrid filter achieved much better noise suppression with minimum edge blurring compared to the original anisotropic diffusion filter when it was tested on an image created based on a molecular image model. The universal quality index, proposed in this paper to measure the effectiveness of denoising, suggests that the anisotropic median-diffusion filter can retain adherence to the original image intensities and contrasts better than other filters. In addition, the performance of the filter is less sensitive to the selection of the image gradient threshold during diffusion, thus making automatic image denoising easier than with the original anisotropic diffusion filter. The anisotropic median-diffusion filter also achieved good denoising results on a piecewise-smooth natural image and real Raman molecular images.

Keywords

molecular imaging, image enhancement, nonlinear filter, anisotropic diffusion

I. INTRODUCTION

Molecular imaging techniques such as fluorescent imaging, isotope radiation imaging, Raman imaging, and positron emission imaging are becoming increasingly important for visualizing and analyzing biophenomena. Molecular imaging makes it possible to visualize the distributions of interesting molecules or chemicals, which are transparent using other modalities. It also becomes possible to measure quantitative information, such as the molecular concentration. However, because recorded molecular images often suffer from a low SNR, image denoising is an important prelude to visual interpretation or automated analysis. It is highly desirable that the filtering process suppresses the noise, while simultaneously retaining adherence to the original image intensities and contrasts, and in particular, preserving information-bearing structures such as edges. Therefore, quality control in the denoising process is necessary.

The anisotropic diffusion filter, first proposed by Perona and Malik [1], is a nonlinear filter which purports to smooth a noisy image without blurring the edges. The diffusion equation for image u is given by

$$\frac{\partial u}{\partial t} = div\,[c(\nabla u)\cdot\nabla u], \tag{1}$$

Revised, February, 2002

where ∇u is a local image gradient and $c(\nabla u)$ is the diffusion coefficient, which is a function of the local gradient. The anisotropic diffusion filter has been broadly used for edge detection [2-4], image segmentation [5, 6], and noise smoothing [7-15], often yielding better results than traditional filters such as the moving average or median filters or other edge-preserving filters [16].

The idea behind the anisotropic diffusion filter is to evolve from a noisy image $g(x,y)$ a family of increasingly smooth images $u(x,y,t)$, indexed by diffusion parameter t, to estimate the original image. The diffusion coefficient $c(\nabla u)$ in equation (1) is sometimes called the "edge-stopping" function, which largely dictates the behavior of the filter. The diffusion coefficient is set such that the filter in equation (1) diffuses the image more in smooth areas and less near the edges. The diffusion coefficient has an argument, the local image gradient, which measures the local edge strength. However, the response of the gradient to the noise element may compete with or exceed the edge response, in which case the diffusion function cannot distinguish between image structure and noise contribution. Therefore, the basic anisotropic diffusion filter in equation (1) usually fails to deliver adequate results in low SNR images; the result either fails to eliminate noise, or leaves the edges significantly blurred [13, 17].

In this paper, we propose an *anisotropic median-diffusion* filter which is specifically intended for denoising low SNR images, and which is particularly suitable for piecewise smooth images such as those encountered in molecular imaging. In Section II, a molecular image model is described. Based on this model, a cell phantom is created as the test image for the modified anisotropic diffusion filter. Section III proposes the use of the *universal image quality index* [18] to measure the effectiveness of image denoising. The anisotropic median-diffusion filter is presented in Section IV. Comparisons of this modified filter with the traditional anisotropic diffusion filter are given in Section V. Finally, the conclusion and remarks are included in Section VI.

II. MOLECULAR IMAGE MODEL

A molecular image illustrates the distribution of a certain molecule. Since the molecules are usually limited within certain areas, a molecular image can often be divided into several regions. A region with a high molecular concentration appears bright while regions with low molecular concentration appear dark. The intensity within a region usually changes gradually while the average intensities between the different regions are quite dissimilar. For such an image, we can use a piecewise-smooth model to describe it, which we will write as

$$f(x,y)=\sum_{i}^{n} s_i(x,y), \tag{2}$$

where the $s_i(x,y)$ indicates a smooth region of $f(x,y)$.

We create a 128x128-pixel phantom according to the model. This phantom, illustrated in figure 1, represents a molecular image of a cell. In the phantom, the image is divided into five regions: the background, the cytoplasm, the nucleus, the mitochondria, and the endoplasmic reticulum (ER). In the phantom we assume the "interesting" molecules are distributed in the cell nucleus, mitochondria, and ER regions, but not in the cytoplasm region. The concentration of the molecules in the nucleus region is Gaussian distributed. The concentration of the molecules in the ER region is linearly distributed, with the highest concentration at the right end. The concentration of the molecules in the mitochondria region is uniform. The entire image has a Gaussian distributed background illumination.

A (noiseless) piecewise-smooth image is usually insensitive to a median filter. This is because a median filter eliminates primarily sudden, transient spikes, while leaving sudden, sustained edges undisturbed. Moreover, the median filter does not significantly perturb the intensities in smooth regions. Figure 2 shows the result of the piecewise image shown in figure 1 following filtering by a 3x3 median filter. Except at the corners of the ER and mitochondria regions, no features in this piecewise-smooth image were corrupted by the median filter. The quality index Q (discussed in Section III) of the filtered image relative to the original image is 0.997 (on a range from -1 to 1, where 1 is the best possible). Moreover, the filtered image does not degrade much if the median filter is applied repetitively.

III. INDEX FOR MEASURING THE QUALITY OF DENOISE FILTER

A simple noise model is used in this paper. A recorded molecular image $g(x,y)$ is assumed to be corrupted by a zero mean Gaussian white noise $n(x,y)$:

$$g(x,y)= f(x,y)+n(x,y). \tag{3}$$

The goal of a denoising filter is to estimate an image $u(x)$ from the $y(x)$ such that the $u(x)$ is as close to the original image $f(x)$ as possible. Many indices have been proposed to measure the efficiency of a denoising filter. The most popular are the mean square error (MSE), the mean absolute error (MAE), the signal-to-noise ratio (SNR), and the peak signal-to-noise ratio. Recently, Wang and Bovik [18] proposed a universal image quality index (Q) that

demonstrates a much better correlation with subjective quality as measured on human subjects. The index Q between the estimated image u and the original image f is quite simply defined as:

$$Q = Q_1 \cdot Q_2 \cdot Q_3, \quad and \tag{4}$$

$$Q_1 = \frac{\sigma_{fu}}{\sigma_f \sigma_u}, \quad Q_2 = \frac{2\mu_f \mu_u}{(\mu_f)^2 + (\mu_u)^2}, \quad Q_3 = \frac{2\sigma_f \sigma_u}{\sigma_f{}^2 + \sigma_u{}^2}, \tag{5}$$

where μ_f and μ_u are the local image means in f and u and where and σ_f^2 , σ_f^2 , and σ_{fu} are local variances and covariances of f and u, respectively. The first item Q_1 measures the degree of local linear correlation between f and u; the second item Q_2 measures the similarity of the mean luminance between f and u; and the third item Q_3 measures the resemblance of the local contrast between the two images. The dynamic range of Q is between [-1, 1]. The best value of 1 is achieved only when $u = f$ locally.

The three components of Q provide a complete profile of the local quality of a denoising filter. In practice, Qs are first estimated in local regions using a sliding window and then combine together to create an overall global image index. Therefore, Q is very sensitive to local, transient image degradations, as well as to global degradations.

IV. THE ANISOTROPIC MEDIAN-DIFFUSION FILTER

A discrete form of the anisotropic diffusion filter described in equation (1) was proposed by Perona and Malik [1] as follows:

$$u_{i,j}^{n+1} = u_{i,j}^{n} + \lambda/4 \cdot \left[c_N \cdot \nabla_N u + c_S \cdot \nabla_S u + c_E \cdot \nabla_E u + c_W \cdot \nabla_W u\right]_{i,j}^{n}, \tag{6}$$

where $\lambda \in [0,1]$ controls the rate of diffusion. Usually a small value λ is used to avoid destabilizing the diffusion process. The letters N, S, E, W (north, south, east and west) describe the direction of the local gradient. The local gradient is calculated using nearest-neighbor differences:

$$\begin{aligned} \nabla_N u_{i,j} &= u_{i-1,j} - u_{i,j} \\ \nabla_S u_{i,j} &= u_{i+1,j} - u_{i,j} \\ \nabla_E u_{i,j} &= u_{i,j+1} - u_{i,j} \\ \nabla_W u_{i,j} &= u_{i,j-1} - u_{i,j} \end{aligned} \tag{7}$$

Research in the anisotropic diffusion filter has been oriented toward understanding the characteristics of the diffusion coefficient $c(\nabla u)$ and then improving the performance of the diffusion filter [19-22]. In this paper, we use

the *Tukey biweight norm* as the diffusion coefficient proposed by Black *et al.* [22]. The normalized (magnitude) Tukey biweight diffusion coefficient is defined as:

$$c(\nabla u, K) = \begin{cases} \frac{25}{16K}\left[1 - \left(\nabla u / \sqrt{5}K\right)^2\right]^2 & |\nabla u| \le \sqrt{5}K \\ 0 & otherwise \end{cases} \qquad (8)$$

where K is a constant that is tuned for a particular application. This constant is the threshold of the local gradients, and determines if a local edge is detected. The *flux function* $\phi(\nabla u)$ is defined as:

$$\phi(\nabla u, K) = c(\nabla u, K) \cdot \nabla u . \qquad (9)$$

The diffusion coefficient and the flux function are plotted in figure 3. This figure together with equations (6) and (7) suggests that when the local gradient between a current pixel and its neighborhood pixel is smaller than the threshold K, the neighborhood pixel is classified as belonging to the same smooth region as the current pixel. Therefore, the neighborhood pixel is actively involved in the smoothing of the current pixel. However, when the local gradient is greater than K but less than $\sqrt{5}K$, the neighborhood pixel is considered to be more distant from the pixel being analyzed in the current smooth region, therefore, such a neighborhood pixel will have less contribution in the smoothing of the current pixel. When the local gradient is greater than $\sqrt{5}K$, the neighborhood pixel is determined to belong to another region, possibly on the other side of an edge. Thus the involvement of this neighborhood pixel in the smoothing is eliminated to avoid edge blurring. Determining a good value of K for a noisy image is critical for the performance of these filters.

Perona and Malik suggested using Canny's "noise estimator" [23] to determine K. Torkamani-Azar and Tait [13] used the mean of the absolute gradient as K. Black *et al.* [22] determined K from the median absolute deviation. All of these methods intend to separate the gradient generated by the noise from the gradient generated by the edges. However, in low SNR images, the average gradient generated by the noise is comparable to or even larger than the edge gradients. Under such a condition, determining a proper K to smooth the noise while retaining the edges is quite difficult. Taking K to be too small will result in a filter that fails to satisfactorily eliminate the overall noise element, especially large noise spikes (see figures 5(b) and 9(b)). Taking K to be large can lead to edge blurring while still failing to reduce large noise spikes (see figures 5(c), 5(d), 9(c) and 10(c)).

We propose to use a median filter in combination with a small K in the diffusion process. In other words, after diffusion via equation (6), a median operation (defined as follows) is used to remove large noise spikes:

$$u_{i,j}^{n+1} = Median(u_{i,j}^{n+1}, W) \tag{10}$$

where W is the window for the median operator (such as a 3x3 square).

This modified anisotropic diffusion filter we call the *anisotropic median-diffusion filter*. With each diffusion step, areas having small gradient are smoothed, while areas with large gradient (from edges or noise spikes) relative to surrounding areas are left unchanged. When the large gradients are generated by large noise spikes, these spikes will be removed effectively by the subsequent median filter. However, if the large gradients are generated by edges, the median filter will not affect them. With each iteration step, low-level noise is smoothed by diffusion, while impulsive noise is removed by the median filter. This process is demonstrated in figure 4. A constant image with unit variance Gaussian noise was created to illustrate the change of the image histogram (or equivalent to noise histogram in this case) with the diffusion steps. The noise histogram (dotted line) after an anisotropic diffusion step indicates that the low-level noise increases and the median-level noise decreases, while the high-level noise remains the same. While the diffusion process smoothes the relative low-level noise, at the same time it equivalently makes the relative high-level noise further "stand out" from the surroundings and thus easily removed by the following median filter. The noise histogram (dashed line) after the subsequent median filter shows that all the relative high-level noise (than surroundings) was greatly eliminated. In a word, the anisotropic diffusion and the median filter work in a complementary way to gradually eliminate the overall noise element without blurring the edges (refer to figures 5(f), 9(d) and 10(d)).

The open-close and close-open filters were suggested by Acton [17] to be used in a way similar to the median filter proposed here. These two morphological filters have the similar function of removing noise spikes. However, they do not perform as well as the median filter in this application (refer to figure 5(e)).

The threshold K in the anisotropic median-diffusion filter is determined with the histogram of the gradient of a noisy image as the reference. However, the anisotropic median-diffusion filter is not sensitive to the exact value of K. As long as K is much less than the standard deviation of the gradient (hopefully less than the edge gradient), while not too small to stop the smoothing process, the denoising results will be similar.

V. EXPERIMENTAL RESULTS AND COMPARISONS

Experiments were carried out on the phantom images with different SNRs. The intensity of the phantom image was normalized into [0,1] for easy comparison. The SNR formula used is:

$$SNR = 20\log_{10}\frac{\sigma[f(x,y)]}{\sigma[n(x,y)]} \tag{11}$$

where $\sigma[f(x,y)]$ and $\sigma[f(x,y)]$ indicate the standard deviations of the original image $f(x,y)$ and noise $n(x,y)$, respectively.

Figure 5 compares the denoising capability with different anisotropic diffusion filters. The degraded image is shown in figure 5(a) with the SNR of 5 dB. Figure 6 is the histogram of the gradient throughout the image in 5(a). As expected, there is no way to separate the gradient of the edges from the gradient of the noise. The standard deviation of the gradient is 0.19. Figures 5(b), 5(c), and 5(d) illustrate images filtered using the traditional anisotropic diffusion filter with different K values. In figure 5(b) K is set to 0.09, which is approximately half of the standard deviation of the gradient. This filtered image shows both impulsive noise spikes and large "noise spots," which are due to improper smoothing of impulsive noise. In figure 5(c) K is set to 0.19, which is the standard deviation of the gradient. The filtered image removed most of the impulsive noise spikes but not the large "noise spots." In addition, edge blurring becomes evident. When K = 0.38, which is twice the standard deviation of the gradient, the edge blurring becomes significant. The big "noise spots" still remain in the filtered result. Clearly, traditional anisotropic diffusion filtering does not deliver adequate results in low-SNR images such as these.

A pair of open-close and close-open filters (alternatively used in the diffusion) was used to smooth the image in figure 5(a) as proposed in [17]. The filtered image in Figure 5(e) shows an obvious illumination distortion relative to the original image. In addition, several "noise spots" still remain on the filtered image. The trend of quality indexes Q, Q_1, Q_2, and Q_3 versus iterations is illustrated in figure 7. The plot of Q_2 obviously illustrates that the mean illumination became worse after using the open-close/close-open diffusion filter.

Figure 5(f) illustrates the results obtained using the anisotropic median-diffusion filter, where K = 0.03, which is much smaller than the standard deviation of the gradient. This image yields an excellent estimate of figure 1. The quality indexes achieved by the different filters are compared in Table 1. Figure 8 illustrates the trend of quality indexes Q, Q_1, Q_2, and Q_3 versus iteration number. In contrast to the quality indexes in the open-close/close-open diffusion filter, figure 8 shows that all three quality measurements: correlation, mean luminance and contrast are gradually improved with the progress of iterations.

The anisotropic median-diffusion filter was tested again on the phantom degraded to SNR = 0 dB. Because of the large noise variation in this image, the standard deviation of the gradient is 0.34, larger than that of the 5 dB

SNR image. However, the same *K* value (0.03) was used to smooth the image when using the anisotropic median-diffusion filter. The results shown in figure 9 illustrate improved performance of the anisotropic median-diffusion filter relative to the traditional algorithm. This example also suggests that selection of the threshold *K* is fairly robust, with the filter performance not being very sensitive to changes in *K*. The robustness of the K selection will make it easy for automatic image denoising.

The anisotropic median-diffusion filter was also tested on a piecewise-smooth natural image as shown in figure 10(a). This egg image was degraded to the SNR of 0 dB by adding zero mean Gaussian noise as illustrated in figure 10(b). The result of applying a traditional anisotropic diffusion filter ($K = 0.2$) is shown in figure 10(c). It also displays "noise spots" as in the phantom case. The filtered image using the new filter is much better at noise suppression, as illustrated in figure 10(d).

Table 1. Summary of the Quality Index Q of the filtered image after using different filters

Noisy Images	Filters	K	Iterations	Noisy Image Q Index*	Filtered Image Q Index*
Phantom Image SNR = 5 dB	Traditional anisotropic diffusion	0.09	100	0.18	0.25
	Traditional anisotropic diffusion	0.19	100	0.18	0.38
	Traditional anisotropic diffusion	0.38	100	0.18	0.34
	Anisotropic open-close-diffusion	0.03	100	0.18	0.29
	Anisotropic median-diffusion	0.03	100	0.18	0.68
Phantom Image SNR = 0 dB	Traditional anisotropic diffusion	0.17	200	0.11	0.17
	Traditional anisotropic diffusion	0.34	200	0.11	0.30
	Anisotropic open-close-diffusion	0.03	200	0.11	0.13
	Anisotropic median-diffusion	0.03	200	0.11	0.52
Egg Image SNR = 0 dB	Traditional anisotropic diffusion	0.20	100	0.12	0.53
	Anisotropic median-diffusion	0.03	100	0.12	0.66

* The index *Q* was calculated relative to the original images.

Finally, we applied the anisotropic median-diffusion filter on Raman images depicting the drug distribution in single tumor cells [24-25]. Drug distribution in a cell can help to characterize the mechanisms of a drug as well as to evaluate the drug efficacy. Figure 11(a) shows a breast cancer cell that has been exposed to Taxol for one hour (Taxol is an anticancer drug that is often used to treat breast cancer). No drug information is shown in this conventional microscopic image. A Raman image was taken to show the Taxol distribution within the boxed area of the cell. Figure 11(b) illustrates the recorded Raman image, which is very noisy. The traditional anisotropic diffusion filter was first applied to smooth the image with $K = 0.1$. The result is shown in figure 11(c), which still contains impulsive noise spikes. Moreover, the edges were blurred somewhat compared to the filtered image in figure 11(d). However, the smoothed image using the proposed anisotropic median-diffusion filter ($K = 0.02$) in figure 11(d) shows better noise suppression and edge retention.

Figure 12(a) shows another breast cancer cell that has been exposed to Taxol for 1.75 hours. In this experiment, the Raman instrumentation was improved so that the field of view of Raman imaging was increased to cover the whole cell. Figure 12(b) is the corresponding Raman image of the cell to show the Taxol distribution. The traditional anisotropic diffusion filter was first applied to smooth (50 iterations) the image with K = the standard deviation of the image gradient. The result is shown in figure 12(c), which still contains impulsive noise spikes. The traditional anisotropic diffusion filter was then applied to smooth (still 50 iterations) the image with K = three times of the standard deviation of the image gradient. The result is shown in figure 12(d), which does not contain impulsive noise spikes anymore. However, large “noise spots” remains, which was also seen in the experiment of synthetic images when K was increased. The result of using the proposed anisotropic median-diffusion filter is shown in Figure 12(e) with K = the standard deviation of the image gradient. By only using only five iterations, the smoothing result appears (although no objective criteria is available) better than the results in Figure 12(c) and (d). The smoothed Raman image in Figure 12(e) was further processed by correcting the non-uniform illumination, subtracting the background, deconvoluting the 3-D blurring, and eliminating the fluorescence signal gives the Raman image in Figure 12(f) [25], it shows the Taxol distribution within the cell. This experiment suggests that anisotropic median-diffusion is more efficient than the traditional anisotropic diffusion filter. This advantage could allow the application of diffusion filter extend to video processing.

VI. CONCLUSION

In this paper we have proposed a new anisotropic diffusion filter for denoising low SNR images, which incorporates a median filter into the diffusion step. This hybrid filter apparently achieves much better noise suppression with minimum edge blurring compared to the original anisotropic diffusion filter. A universal quality index suggests that this filter retains adherence to the original image intensities and contrasts better than other filters. In addition, this filter is less sensitive to the selection of the image gradient threshold during diffusion, thus making automatic image denoising easier than with the original anisotropic diffusion filter. This filter is also more efficient than the original anisotropic diffusion filter, thus making the application of diffusion filter in video processing feasible. This new filter is particularly useful for low-SNR molecular images such as fluorescence, Raman, isotope radiation and positron emission images.

References

[1] P. Perona and J. Malik, "Scale-space and edge detection using anisotropic diffusion," *IEEE Transactions on Pattern Analysis & Machine Intelligence*, vol. 12, pp. 629-39, 1990.

[2] S. T. Acton, "Edge enhancement of infrared imagery by way of the anisotropic diffusion pyramid," *Proceedings. International Conference on Image Processing (Cat. No.96CH35919). IEEE. Part vol.1, 1996*, pp. 865-8 vol.

[3] G. Gallo, A. Zingale, and R. Zingale, "Detection of MRI brain contour using nonlinear anisotropic diffusion filter," *Proceedings of the 18th Annual International Conference of the IEEE Engineering in Medicine and Biology Society. `Bridging Disciplines for Biomedicine' (Cat. No.96CH36036). IEEE. Part vol.3, 1997*, pp. 1062-4 vol.

[4] M. Garcia-Silvente, J. A. Garcia, J. Fdez-Valdivia, and A. Garrido, "A new edge detector integrating scale-spectrum information," *Image and Vision Computing*, vol. 15, pp. 913-923, 1997.

[5] S. T. Acton, A. C. Bovik, and M. M. Crawford, "Anisotropic diffusion pyramids for image segmentation," *Proceedings ICIP-94 (Cat. No.94CH35708). IEEE Comput. Soc. Press. Part vol.3, 1994*, pp. 478-82 vol.

[6] J. Maeda, T. Iizawa, T. Ishizaka, C. Ishikawa, and Y. Suzuki, "Segmentation of natural images using anisotropic diffusion and linking of boundary edges," *Pattern Recognition*, vol. 31, pp. 1993-1999, 1998.

[7] Y. L. You and M. Kaveh, "Fourth-order partial differential equations for noise removal," *IEEE Transactions of Image Processing*, vol. 9, pp. 1723-30, 2000.

[8] L. Zhouchen and S. Qingyun, "An anisotropic diffusion PDE for noise reduction and thin edge preservation," *Proceedings 10th International Conference on Image Analysis and Processing. IEEE Comput. Soc. 1999*, pp. 102-7.

[9] I. Bajla and M. Sramek, "Improvement of 3D visualization of the brain using anisotropic diffusion smoothing of MR data," *International Journal of Healthcare Technology & Management*, vol. 1, pp. 390-400, 1999.

[10] J. Monteil and A. Beghdadi, "A new adaptive nonlinear anisotropic diffusion for noise smoothing," *Proceedings 1998 International Conference on Image Processing. ICIP98 (Cat. No.98CB36269). IEEE Comput. Soc. Part vol.3, 1998*, pp. 254-8 vol.

[11] Y. M. Chen, B. C. Vemuri, and L. Wang, "Image denoising and segmentation via nonlinear diffusion," *Computers & Mathematics with Applications*, vol. 39, pp. 131-149, 2000.

[12] S. H. Lee, M. G. Kang, and K. T. Park, "CCD noise filtering based on 3-dimensional nonlinear partial differential equation," *IEEE Transactions on Consumer Electronics*, vol. 44, pp. 1086-1090, 1998.

[13] F. Torkamani-Azar and K. E. Tait, "Image recovery using the anisotropic diffusion equation," *IEEE Transactions of Image Processing*, vol. 5, pp. 1573-8, 1996.

[14] G. Gerig, O. Kubler, R. Kikinis, and F. A. Jolesz, "Nonlinear Anisotropic Filtering of MRI Data," *IEEE Transactions on Medical Imaging*, vol. 11, pp. 221-232, 1992.

[15] P. J. Verveer, M. J. Gemkow, and T. M. Jovin, "A comparison of image restoration approaches applied to three- dimensional confocal and wide-field fluorescence microscopy," *Journal of Microscopy-Oxford*, vol. 193, pp. 50-61, 1999.

[16] J. Ling and A. C. Bovik, "Modeling and Restoration of Raman Microscopic Images," presented at IEEE 2000 International Conference on Image Processing (ICIP), Vancouver, Canada, 2000.

[17] S. T. Acton, "Diffusion-Based Edge Detectors," in *Handbook of Image & Video Processing*, A. C. Bovik, Ed. San Diego: Academic Press, 2000, pp. 433-447.

[18] Z. Wang and A. C. Bovik, "A Universal Image Quality Index," *Submitted to IEEE Signal Processing Letters*, 2001.

[19] G. Aubert and L. Vese, "A variational method in image recovery," *Siam Journal on Numerical Analysis*, vol. 34, pp. 1948-1979, 1997.

[20] S. Kichenassamy, "The Perona-Malik paradox," *Siam Journal on Applied Mathematics*, vol. 57, pp. 1328-1342, 1997.

[21] Y. L. You, W. Y. Xu, A. Tannenbaum, and M. Kaveh, "Behavioral analysis of anisotropic diffusion in image processing," *IEEE Transactions on Image Processing*, vol. 5, pp. 1539-1553, 1996.

[22] M. J. Black, G. Sapiro, D. H. Marimont, and D. Heeger, "Robust anisotropic diffusion," *IEEE Transactions on Image Processing*, vol. 7, pp. 421-432, 1998.

[23] J. Canny, "A computational approach to edge detection," *IEEE Transactions on Pattern Analysis & Machine Intelligence*, vol. PAMI-8, pp. 679-98, 1986.

[24] J. Ling, R. V. Moore, M. Miller, A. C. Bovik, and S. D. Weitman, "Application of Raman Imaging Microscopy to Evaluate Drug Distribution within Cancer Cells," presented at 91st Annual Meeting of American Association for Cancer Research, San Francisco, California, 2000.

[25] J. Ling, *The Development of Raman Imaging Microscopy To Visualize Drug Actions in Living Cells*, Ph.D. Dissertation in Department of Biomedical Engineering. 2001, The University of Texas at Austin: Austin.

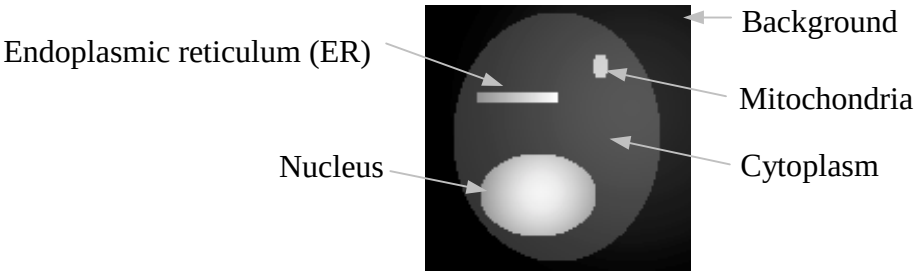

Figure 1. A phantom to represent a cellular molecular image.

Figure 2. The result of the phantom in figure 1 filtered by a 3x3 median filter.

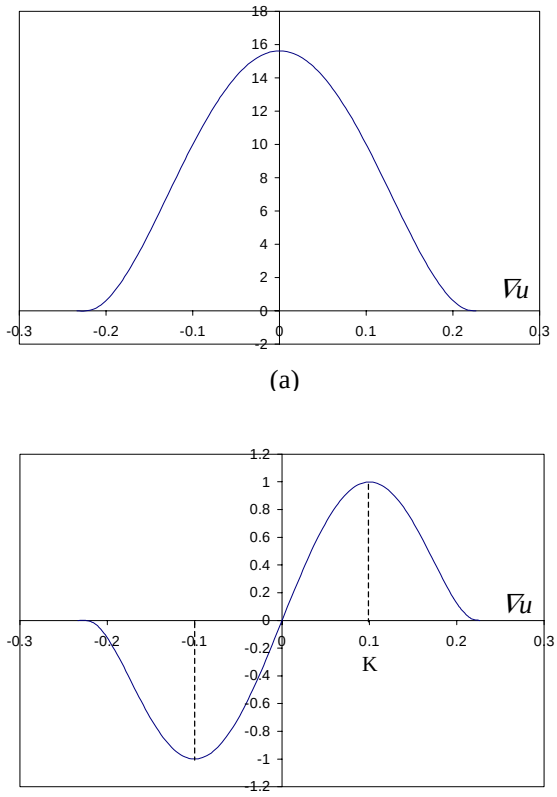

Figure 3. The diffusion function (a, Eq. 8) and the normalized flux function (b, Eq. 9) with $K = 0.1$.

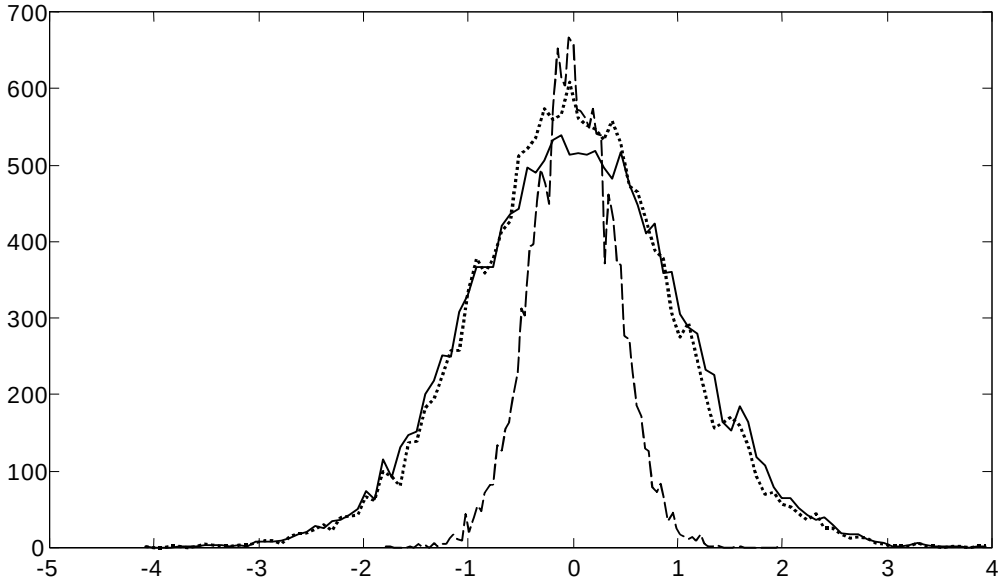

Figure 4. Histogram change of a constant image plus Gaussian noise (with unit variance) during anisotropic median-diffusion. Solid line: the original histogram of the Gaussian noise image. Dotted line: the histogram after the first anisotropic diffusion step. Dashed line: the histogram after the subsequent median filter.

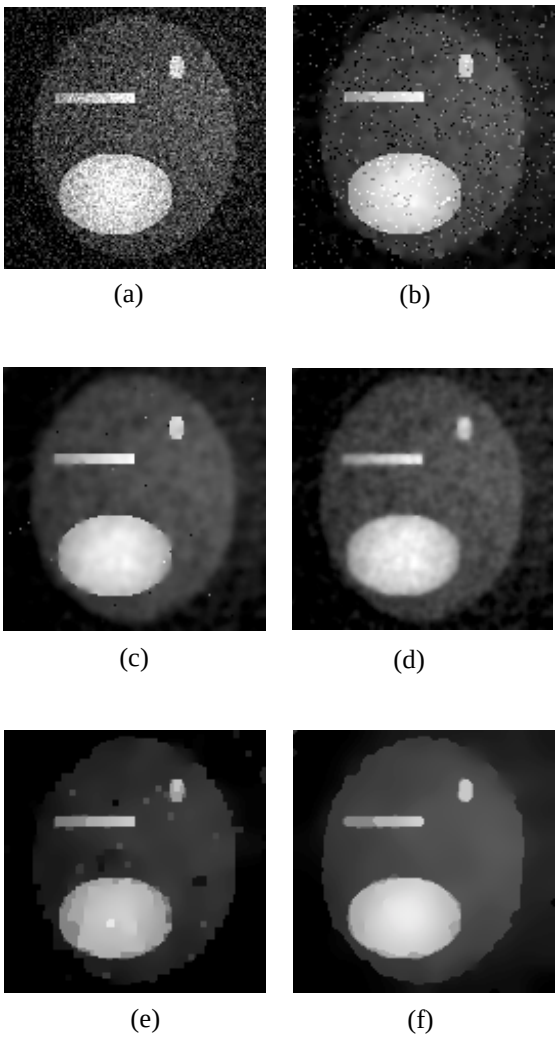

Figure 5. Low SNR image denoising using different anisotropic diffusion filters. (a) phantom from figure 1 degraded SNR = 5 dB. (b), (c), (d) filtered images using traditional anisotropic diffusion filter with K = 0.09, 0.19, and 0.38, respectively. (e) filtered image using anisotropic open-close-diffusion filter with a 3x3 window, where K = 0.03. (f) filtered image using anisotropic median-diffusion filter with a 3x3 window, where K = 0.03. All the filters run 100 iterations in the diffusion.

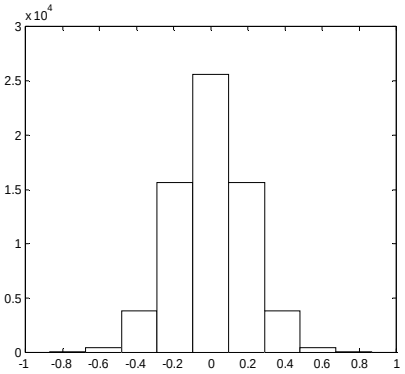

Figure 6. Histogram of the gradient for the noisy image in figure 5(a)

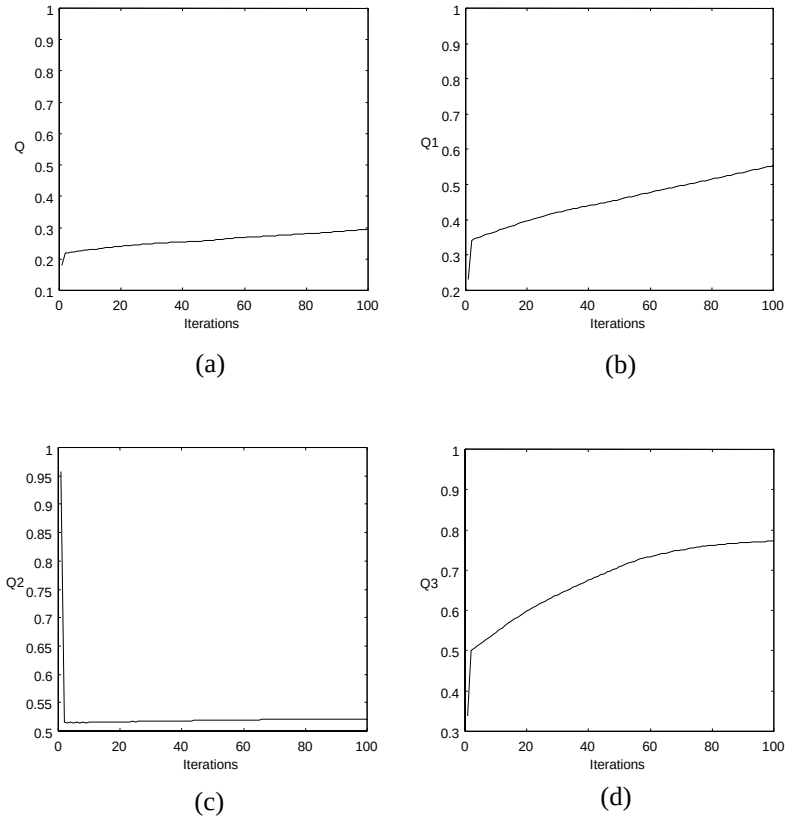

Figure 7. Quality indexes (a) Q, (b) Q_1, (c) Q_2 and (d) Q_3 vs. iteration number during smoothing of the image in figure 5(a) with the anisotropic open-close-diffusion filter.

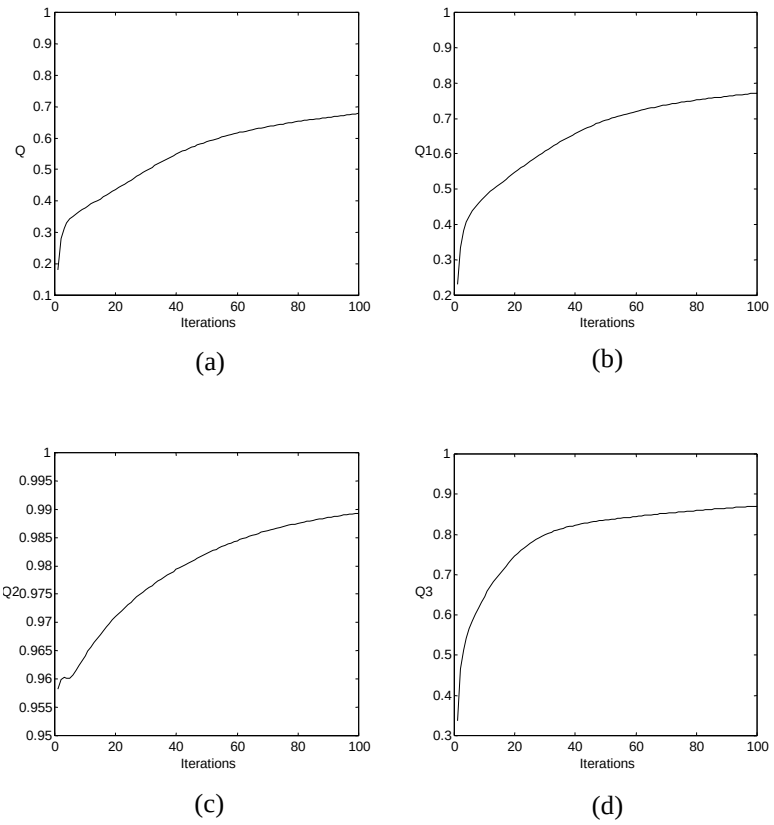

Figure 8. Quality indexes (a) Q, (b) Q_1, (c) Q_2 and (d) Q_3 vs. iteration number during smoothing of the image in figure 5(a) with the anisotropic median-diffusion filter.

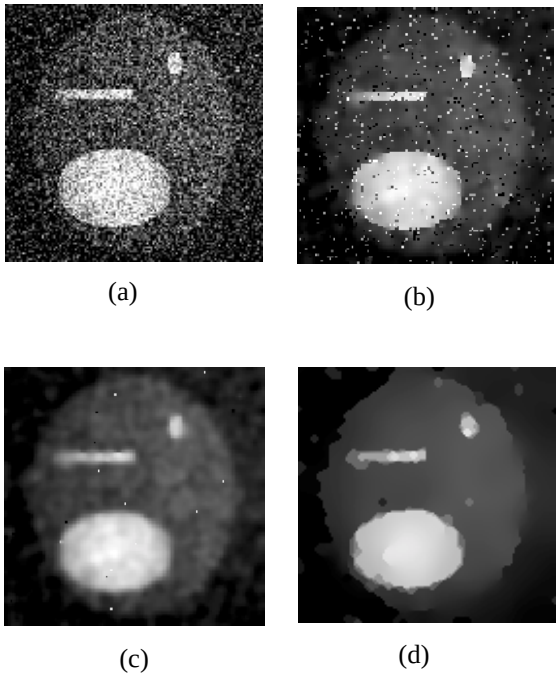

Figure 9. (a) phantom shown in figure 1 degraded to SNR = 0 dB. (b), (c) filtered images using traditional anisotropic diffusion filter with K = 0.17, 0.34, respectively. (d) filtered image using the anisotropic median-diffusion filter with a 3x3 window, where K = 0.03. All the filters run 200 iterations in the diffusion.

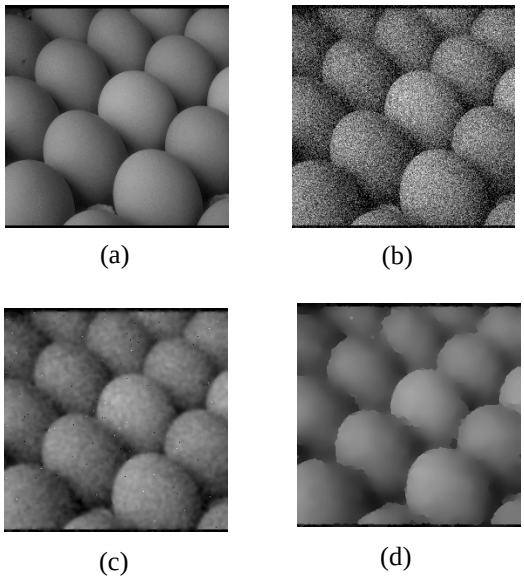

Figure 10. (a) natural piecewise smooth image of eggs. (b) image in (a) degraded to 0 dB SNR. (c) filtered image using traditional anisotropic diffusion filter with K = 0.2. (d) filtered image using anisotropic median-diffusion filter with a 3x3 window and K = 0.03. The filters run 100 iterations in the diffusion.

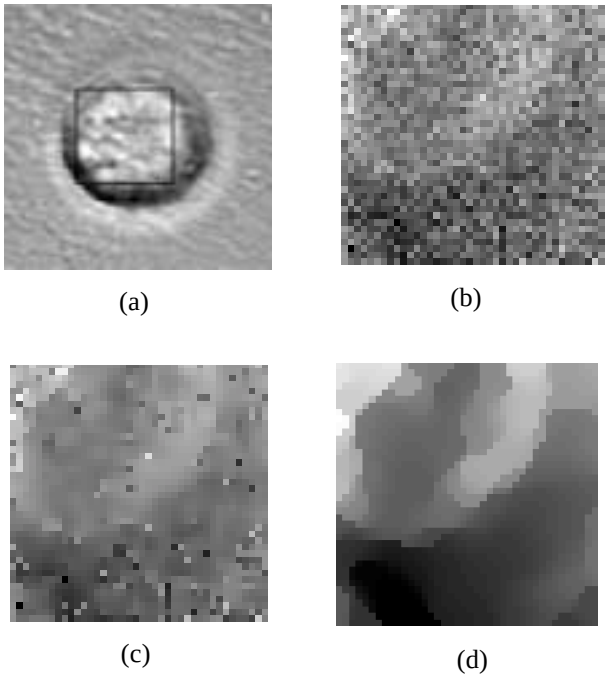

Figure 11. (a) Conventional microscopic image of a breast cell which has been exposed to Taxol for one hour. (b) The recorded Raman image corresponding to the boxed area of the cell. (c) filtered image using traditional anisotropic diffusion filter with K = 0.1. This filter ran 20 iterations in the diffusion. (d) filtered image using anisotropic median-diffusion filter with a 3x3 window and K = 0.02. This filter ran 10 iterations in the diffusion.

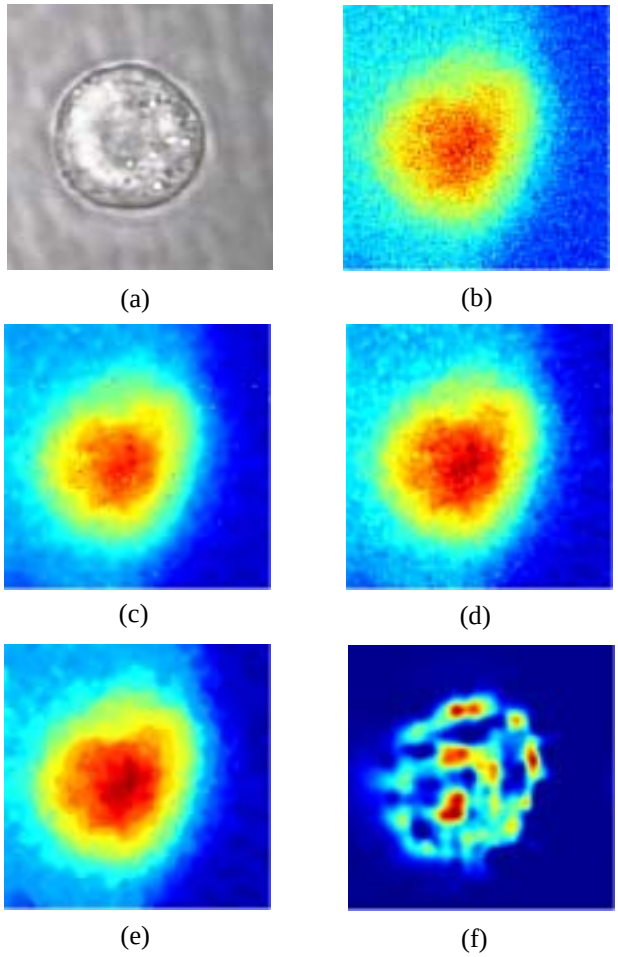

Figure 12. (a) Conventional microscopic image of a breast cell which has been exposed to Taxol for 1.75 hours. (b) The recorded Raman image corresponding to the cell. (c) filtered image using traditional anisotropic diffusion filter with K = the standard deviation of the image gradient. This filter ran 50 iterations in the diffusion. (d) filtered image using traditional anisotropic diffusion filter with K = three times the standard deviation of the image gradient. This filter ran 50 iterations in the diffusion (e) filtered image using anisotropic median-diffusion filter with a 3x3 window and K = the standard deviation of the image gradient. This filter ran 5 iterations in the diffusion. (f) Raman image shows the Taxol distribution within the cell after further processing (correction of the non-uniform illumination, subtract background, 3-D deconvolution, and eliminate fluorescence signal) the Raman image in (e).